

In vivo monitoring of drought-induced embolism in *Callitris rhomboidea* trees reveals wide variation in branchlet vulnerability and high resistance to tissue death

Kate M. Johnson , Christopher Lucani  and Timothy J. Brodribb 

Discipline of Biological Sciences, School of Natural Sciences, University of Tasmania, Private Bag 55, Hobart, TAS 7001, Australia

Summary

Authors for correspondence:

Timothy J. Brodribb

Email: timothy.brodribb@utas.edu.au

Kate M. Johnson

Email: kate.johnson@utas.edu.au

Received: 1 July 2021

Accepted: 1 October 2021

New Phytologist (2022) **233**: 207–218

doi: [10.1111/nph.17786](https://doi.org/10.1111/nph.17786)

Key words: *Callitris rhomboidea*, cavitation, conifer, drought, embolism, fluorescence, vulnerability, xylem.

- Damage to the plant water transport system through xylem cavitation is known to be a driver of plant death in drought conditions. However, a lack of techniques to continuously monitor xylem embolism in whole plants *in vivo* has hampered our ability to investigate both how this damage propagates and the possible mechanistic link between xylem damage and tissue death.
- Using optical and fluorescence sensors, we monitored drought-induced xylem embolism accumulation and photosynthetic damage *in vivo* throughout the canopy of a drought-resistant conifer, *Callitris rhomboidea*, during drought treatments of c. 1 month duration.
- We show that drought-induced damage to the xylem can be monitored *in vivo* in whole trees during extended periods of water stress. Under these conditions, vulnerability of the xylem to cavitation varied widely among branchlets, with photosynthetic damage only recorded once > 90% of the xylem was cavitated.
- The variation in branchlet vulnerability has important implications for understanding how trees like *C. rhomboidea* survive drought, and the high resistance of branchlets to tissue damage points to runaway cavitation as a likely driver of tissue death in *C. rhomboidea* branch tips.

Introduction

Acute water deficit kills trees of all species and ages, and though recent research provides insights into how this occurs, we are still far from fully understanding the primary mechanisms driving drought-induced tree death. With forest dieback increasing across the world and predictions of more frequent and severe drought events, understanding how trees die in drought is a priority for research owing to the many irreplaceable roles that trees play in climatic regulation and terrestrial processes (Allen *et al.*, 2010; Choat *et al.*, 2012; McDowell *et al.*, 2013, 2020; Hoegh-Guldberg *et al.*, 2018; Brodribb *et al.*, 2020). Recent studies have revealed the sequence of events within a plant that lead to drought-induced plant death (Preisler *et al.*, 2020; Wang *et al.*, 2021) and identified thresholds beyond which plants and plant organs are unlikely to, or cannot, recover. These relate to both failure of the plant water transport system ultimately leading to tissue desiccation and death (Hammond *et al.*, 2019; Brodribb *et al.*, 2021) and tissue desiccation itself (Johnson *et al.*, 2018; Lamacque *et al.*, 2020; Preisler *et al.*, 2020). Though this information provides insights into the processes that lead to plant death, an inability to continuously monitor xylem damage *in vivo* has made it challenging to determine how this process is associated with tissue damage and death in whole trees.

Damage to the plant water transport system (xylem) is often implicated as a driver of drought-induced plant death because tree survival is dependent upon an uninterrupted supply of water to leaves through the xylem. The movement of water from the roots to the leaves is driven by a gradient in water tension, where evaporating water from the leaves causes increasing tension (increasingly negative water potential) in the canopy, driving the flow of water from the roots to the leaves. This tension increases under drought conditions; and when it exceeds a threshold, air can rapidly enter the xylem through porous structures (pits) in conduit walls, where it expands rapidly to fill the conduit. This process is called xylem cavitation, resulting in air bubbles called xylem embolisms (Lewis, 1988; Tyree & Sperry, 1988). With continued drying, cavitation can lead to complete blockage of the water transport system with air and plant death (Tyree & Sperry, 1988; Choat *et al.*, 2012). Determining thresholds of water stress (associated with the extent of embolism) beyond which damage and death will occur is critical for predicting when different organs, and ultimately the whole tree, will die in drought conditions. Knowledge of these thresholds or the probability of death at certain thresholds (Hammond *et al.*, 2019) can be combined with knowledge of the climatic conditions that induce these, allowing prediction of conditions likely to lead to death in drought (Blackman *et al.*, 2012, 2016; Skelton *et al.*, 2015; Larter *et al.*, 2017; Martin-StPaul, 2017).

A number of embolism thresholds have been correlated with drought-induced death of plants and plant organs, ranging from 50% xylem damage in both conifers (Brodrribb & Cochard, 2009; Choat *et al.*, 2012; Larter *et al.*, 2017) and angiosperms (Choat *et al.*, 2012; Liang *et al.*, 2021) to 88% in angiosperms, both woody (Urli *et al.*, 2013) and herbaceous (Skelton *et al.*, 2017). However, these thresholds do not necessarily explain a mechanistic link between embolism and death. The water potentials associated with 12%, 50%, and 88% embolism (known as the P12, the P50, and P88, respectively) are commonly reported numbers used to make comparisons between the embolism resistance of different plants and organs. However, the relationships between these thresholds and plant death are based on correlation rather than causation. For example, while the water potential that induces 50% loss of water transport capacity in the stem xylem due to air embolism in trees has been correlated with drought mortality (Brodrribb & Cochard, 2009; Choat *et al.*, 2012; Choat, 2013), 50% loss of stem water conductivity is unlikely to cause lethal dehydration of tissues. This is because 50% of the xylem is capable of maintaining hydration of branches with substantially reduced gas exchange (Dietrich *et al.*, 2018).

The concept of a lethal water potential threshold, associated with a percentage of xylem embolism, is based on the idea that, in severe drought conditions, loss of water from the leaf surface can destabilize the relatively homeostatic water balance within the plant. Stomatal closure at the leaf surface is one of the first plant responses to water deficit and has been shown to precede cavitation in many plant species (Brodrribb & McAdam, 2017; Martin-StPaul, 2017), such as olive (Rodríguez-Domínguez & Brodrribb, 2020), grape vines (Hochberg *et al.*, 2017), and hundreds of species from across diverse biomes (Martin-StPaul, 2017). However, water is also lost through incompletely closed stomata (Duursma *et al.*, 2019) and through the cuticle (Becker *et al.*, 1986; Lenzian & Kerstiens, 1991; Kerstiens, 1996). Though this loss of water is small, it is a critically important factor in determining drought survival (Blackman *et al.*, 2016; Martin-StPaul, 2017; Márquez *et al.*, 2021). Water loss through cuticular leakiness can cause a local drop in plant water potential in the leaves, inducing cavitation and leading to a further drop in water potential in a positive feedback loop that results in uncontrolled cavitation and tissue death. This process, called ‘runaway cavitation’ (Milburn, 1973; Tyree & Sperry, 1988), ultimately leads to lethal tissue desiccation. As the water loss in drought-affected leaves is low, a high percentage of embolism is likely required for this positive feedback to be triggered. Runaway cavitation is likely to occur first in the leaves (Brodrribb *et al.*, 2021) at the site of evaporative water loss, where the resistance to water flow is high. Leaves have also been shown to be more vulnerable than stems in angiosperms (Charrier *et al.*, 2016; Skelton *et al.*, 2019) and conifers (Brodrribb & Cochard, 2009), suggesting that they may become disconnected from the plant vascular system early in drought events, making the leaves an ideal site to study the mechanistic relationship between embolism and tissue death in trees.

Though studies of excised plant organs have allowed us to quantify the drought resistance of many plant species, enabling both within and between-species comparisons of drought

vulnerability, the emergence of techniques to monitor failure of the plant water transport system *in vivo* has been a key innovation for understanding how the plant water transport system behaves under drought conditions. These techniques include the use of X-rays (micro computed tomography (micro-CT)) and visible light (the optical technique) to monitor embolism (Zhang & Brodrribb, 2017; Rodríguez-Domínguez *et al.*, 2018; Bourbia *et al.*, 2020). Micro-CT has been used to image xylem embolism in whole, intact plants (Choat *et al.*, 2015, 2016; Cochard *et al.*, 2015; Gauthey *et al.*, 2020), providing high-resolution spatial information with three-dimensional images, but repeated scanning has been shown to damage plant tissue and cannot be performed continuously during long-term dehydration (Cochard *et al.*, 2015; Nardini *et al.*, 2017; Petruzzellis *et al.*, 2018). Also, owing to the limited access to micro-CT facilities in terms of both frequency of access and length of allocated time, compared with the long time period required to impose water stress that mimics natural drought, it is not currently feasible to use micro-CT for monitoring in long-term drought experiments (Nolf *et al.*, 2017). The recently developed optical vulnerability technique (OVT; Brodrribb *et al.*, 2016a) presents a potentially accessible way to monitor embolism with high temporal resolution through continuous image capture in whole plants (Brodrribb *et al.*, 2016a; Rodríguez-Domínguez *et al.*, 2018; Gauthey *et al.*, 2020; Johnson *et al.*, 2020). This creates an opportunity to study cavitation over extended periods in intact trees without causing significant damage to plant tissues.

Here, we used the OVT to quantify drought-induced embolism spread throughout the canopies of potted individuals of the gymnosperm species *Callitris rhomboidea*. We paired this with measurements of Chl fluorescence, made before and after exposing trees to drought treatments, to assess tissue damage in the branchlets we monitored for embolism. We aimed to determine how embolism spreads through the intact canopy of *C. rhomboidea* saplings, and whether tissue damage in leaves is associated with a very high percentage of embolism during drought, as expected if runaway cavitation is the trigger. By monitoring xylem embolism *in vivo* in whole plants, droughted gradually over a period of 2–3 wk, we hoped to understand if a mechanistic connection between cavitation and canopy death exists in trees during drought events.

Materials and Methods

Drought experiment

Four 3-yr-old *C. rhomboidea* saplings, grown under ambient conditions in Hobart (42.8826°S, 147.3257°E) in 2 l pots in a fine pine bark, were placed in a temperature-controlled glasshouse (daytime temperature 25°C, night-time temperature 15°C, 50% relative humidity). Trees were acclimated under these conditions for *c.* 2 wk. This species was chosen owing to its drought resistance and the extensive body of drought research on this species and the *Callitris* clade (Heady *et al.*, 1994; Brodrribb & Cochard, 2009; Pittermann *et al.*, 2010; Bouche *et al.*, 2014; Larter *et al.*, 2017; Bourbia *et al.*, 2021). With a water transport system

constituting the typical ‘homoxylous’ wood of gymnosperms, we expect that the results of this study could be extrapolated to other gymnosperm species.

The *C. rhomboidea* trees ranged from 1 to 1.8 m in height. Five branchlets per tree, ranging from 30 cm above the soil to the tips of the trees, were selected for optical visualization of embolism. A sharp razor was used to remove *c.* 5 mm² of bark from one side of a stem *c.* 1–2 mm in diameter (ensuring that at least 50% of phloem remained intact). A hydrogel (Tensive Gel; Parker Laboratories Inc., Fairfield, NJ, USA) was applied to the exposed xylem to reduce surface evaporation and improve light transmission. A Raspberry Pi-based time-lapse camera with $\times 30$ magnification and LED illumination (MiCAMs, also known as ‘cavicams’; <https://micams.co>) were attached to each of the five branchlets. An ICT stem psychrometer (ICT PSY, Armidale, NSW, Australia) was mounted on the main stem near the base of the tree and shielded with bubble wrap, foil, and heat-reflecting material to minimize fluctuations in water potential measurements due to heating and cooling of the instrument (Fig. 1). Water was withheld from the trees while MiCAMs recorded images continuously, at 3-min intervals (Supporting Information Video S1) for the duration of the experiment. The ICT stem psychrometer recorded water potential every 10 min. Midday water potential was measured using branch tips, *c.* 2–3 cm in length using a Scholander pressure bomb every 3 d to validate psychrometer readings and captured images were checked frequently for evidence of embolism and to correct camera focus as required.

Each of the four trees was dried to a target level of drought stress, which took 2–3 wk per tree (Fig. S1). The drought stress treatments were determined with reference to the published P50 of *C. rhomboidea* branches (–10 MPa) and the equivalent of the

small stems measured here (–6 MPa) (Brodribb & Cochard, 2009). The predawn water potential was used to determine when the level of stress was reached. Target levels of drought stress were a mild treatment not expected to cause stem cavitation (between –4 and –5 MPa), a moderate treatment expected to initiate stem cavitation in the main stem and most of the canopy (*c.* –7 MPa), and a severe treatment expected to cause extensive stem xylem cavitation (*c.* –9 MPa). The dehydration rate was relatively constant between trees (decreasing by *c.* 0.2 MPa d^{–1}; Fig. S1). As the main aim of this study was to determine whether embolism can be monitored across intact trees, and to subsequently answer a number of questions about how embolism propagates, our replication focused on monitoring many branches per tree rather than replicating the drought stress treatments.

Once the target water potential was reached, trees were rewatered by saturating the pots and leaving the base submerged in a container filled with *c.* 3 mm of water. The pots remained in water for *c.* 24–72 h until main-stem water potential, measured using an ICT stem psychrometer, recovered to close to 0 MPa. The camera-monitored branchlets were then excised and allowed to dehydrate while image capture continued to monitor xylem embolism until all conduits were air filled. This provided a 100% embolism reference by which percentage loss of conductivity could be calculated during drought (Johnson *et al.*, 2018).

Assessing tree health

Fluorescence Eleven branchlets spanning the height of each tree, including the five that were monitored for embolism, were tagged for measurements of photosynthetic function. This was measured by means of Chl fluorescence assessment of maximum photosystem II quantum yield (assessed as the ratio of variable to maximum fluorescence, F_v/F_m , after application of a saturating pulse of light) using a PAM 2000 portable Chl fluorometer (Walz, Effeltrich, Germany). These measurements were taken at branchlet tips treatments (*c.* 2 cm from the absolute branch apex, where tissue growth was expected to have ceased), both before and after drought, since close to the branchlet tips is where we expected to see tissue damage first during drought. Initial fluorescence was measured for each of the 11 branchlets before the drought treatments in well-watered plants after a 2 h dark adaptation period. These measurements were repeated post-drought, on both branchlets still attached to the plant and the recently excised branches with cameras attached. In camera branchlets, the leaves were encased in foil during the 2 h dark adaptation period to ensure that the camera light did not interfere with dark adaptation, and fluorescence was measured immediately downstream of the camera. Branchlet preparation for OVT visualization did not have a significant impact on the photosynthetic efficiency (F_v/F_m) of the leaves downstream of the imaging site (Fig. S2).

Transpiration To determine the effect of the drought treatments on whole tree function, midday canopy transpiration E (mmol m^{–2} s^{–1}) was measured in all trees both before and after the drought treatment. In the days preceding the drought treatment, a sunny day was chosen to ensure that the stomata would

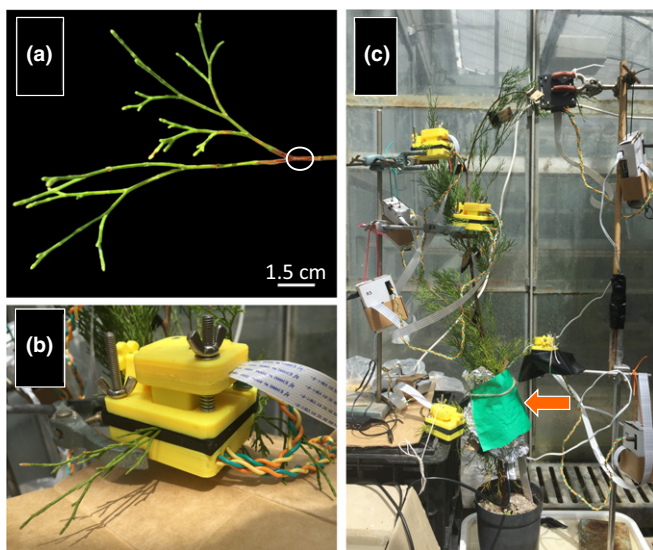


Fig. 1 Set-up for optical embolism monitoring in *Callitris rhomboidea* saplings. (a) A branchlet prepared for embolism monitoring using the optical vulnerability technique, with the exposed xylem indicated by a white circle. (b) A MiCAM attached to a branchlet. (c) A tree with five MiCAMs attached and the shielded ICT stem psychrometer, which is attached to the main stem near the base of the tree (indicated by the orange arrow).

be open and therefore the measurements would likely reflect the trees' maximum transpiration rate. The pot of the sapling was then wrapped in two plastic bags, entirely covering the soil, to ensure that the transpiration measured did not include water loss from the soil. At 11:00 h, plants were placed on a balance (XS6002S, 6100 g \pm 0.01 g; Mettler-Toledo GmbH, Greifensee, Switzerland) in a temperature-controlled glasshouse, where weights were recorded every 10 min. The times and weights were then used to calculate the maximum midday canopy transpiration rate. This was repeated for each plant post-drought treatments, 24–72 h after initial rewatering (when main-stem water potential was close to 0 MPa) and the percentage change in transpiration after drought was calculated.

Xylem vulnerability

The xylem vulnerability of all branchlets was compiled from embolism recorded during whole-plant dehydration along with embolism recorded after branchlet excision. As water potential was measured using a psychrometer attached to the main stem, the water potential of excised branchlets was unknown once the branchlets were severed after drought to allow 100% embolism to be reached. Given the strong correlation between shrinkage of branchlet tissue and water potential in *C. rhomboidea*, as shown recently (Bourbia *et al.*, 2021), we extracted shrinkage and determined the mean relationship between branchlet shrinkage and main-stem water potential in order to predict branchlet water potential beyond branchlet excision (Fig. S3).

Extracting shrinkage

To calibrate the relationship between the main-stem water potential and branchlet shrinkage, the branchlet width was measured daily in the OVT images at predawn (04:00 h) throughout dehydration and rehydration (after rewatering). The width of branchlets (where the initial well-watered width is 100%) was plotted against main-stem water potential at 04:00 h each day (measured using an ICT stem psychrometer). Predawn stem water potentials were used as the stable ambient temperature at this time minimized fluctuation of psychrometer temperature, allowing maximum confidence in the accuracy of the psychrometer water potential readings. As the shrinkage measurements at very hydrated water potentials (less negative than -1 MPa) fluctuated in some branchlets, 100% width was defined as the branchlet width at -1 MPa.

To determine the branchlet water potential post-excision, after the drought treatment the shrinkage was measured in severed branchlets at 8 h intervals (04:00 h, 12:00 h, and 20:00 h) each day until the branchlet width reached a stable minimum (2–7 d). This allowed us to capture the more rapid changes in shrinkage (and therefore water potential) that occurred after branchlet excision. The relationship between stem water potential and branchlet shrinkage prior to excision could then be used to predict branchlet water potential from post-excision shrinkage values.

Breakpoint analysis The relationship between main-stem water potential and branchlet shrinkage across all branches could be

described by a two-phase linear decline (segmented or 'piecewise' regression) (Fig. S4). Using RSTUDIO v.1.1.383, we fitted a generalized additive model (GAM) using the gam function in the MGCV package (Wood, 2011) to describe the mean relationship between stem water potential and branchlet shrinkage for all branchlets and then used the lm.segmented function in package SEGMENTED (Muggeo, 2008) to define the 'breakpoint' water potential, where the slope of mean branchlet shrinkage shifted. In branchlets where P50 and P88 were not reached before rewatering, meaning that the stem water potential values could not be used to complete an entire vulnerability curve, we used the segmented regression (predicted from the GAM as already described herein) to predict branchlet water potential after excision allowing complete curves to be constructed and P50 and P88 to be extracted (Figs S3, S4). While the stem psychrometer monitored water potential continuously, since both the shrinkage measurements and the water potential values used for analysis were not continuous (taken as point measurements at 04:00 h each day), we used linear interpolation to determine the stem water potentials (before rewatering) and shrinkage-predicted water potentials (after branches were cut off) for those images without stem water potential or shrinkage values. By assuming a linear decrease between the known measurements, water potential values were generated for each OVT image using PYTHON v.3.9.1 (Python Software Foundation; van Rossum, 1995) to allow embolism data to be plotted against water potential data both before and after rewatering. The two equations describing the relationship between water potential and shrinkage before and after the calculated breakpoint of -4.38 MPa were used to predict water potential and shrinkage based on the water potential range. Stem water potential values were used where available, after which the shrinkage-predicted water potentials were used (Figs S3, S4).

Image analysis From the OVT images, a 500 px \times 500 px (*c.* 1 mm²) region of interest that remained sharply in focus for the entire image capture duration (20–30 d) was selected for images analysis to extract embolism data. Embolism data for branchlets were only included where there had been no break in image capture and the stem remained within frame from the entire duration of the experiment. This meant that the data for one or two of the five monitored branchlets was excluded in three out of the four trees, resulting in a total sample size of 16 branchlets across the four trees. The changes in light reflection caused by cavitation were highlighted by an image subtraction procedure performed in IMAGEJ (Brodribb *et al.*, 2016a). Any 'noise' associated with gradual changes to the branchlets during drying was removed, leaving only changes in pixel brightness intensity associated with the embolisms resulting from rapid cavitation events (see <http://www.opensourceov.org/> for full details). Embolized pixels were then expressed as a percentage of the total embolized pixel area and plotted against predicted branchlet water potential to construct vulnerability curves.

Hydraulic conductance

To test whether preparation of branchlets for the OVT had an effect on xylem function hydraulic conductance

K ($\text{mmol m}^{-2} \text{s}^{-1} \text{MPa}^{-1}$), a *C. rhomboidea* sapling, of similar age to those used for the drought experiment, was selected and eight branchlets were prepared using the same preparation method used for OVT embolism monitoring (carefully sliced using a sharp razor, as described earlier herein). An ICT stem psychrometer was attached close to the tree's base to monitor stem water potential. The tree was dried to two water potentials, predicted to induce either minimal branchlet embolism or close to 50% branchlet embolism (-2 MPa and -5 MPa, respectively). Once each of the target water potentials was reached, K was measured in three or four OVT-prepared (cut) branchlets and three or four unprepared (uncut) branchlets using a variation of the low-pressure flow meter set-up described in Melcher *et al.* (2012) (Fig. S5). Branchlets *c.* 10 cm in length were excised from the plants and allowed to equilibrate in a sealed plastic bag for *c.* 30 min. Branchlets were then removed from the bag and all stem and leaf tissue upstream of the exposed xylem (or location where the xylem would have been monitored in the case of the uncut branchlets) was carefully excised with a sharp razor blade (Fig. S5). This ensured that the measurements reflected only the K of the tissue downstream of the OVT site, to accurately test whether OVT preparation had an effect on branch water supply downstream of the OVT preparation. Branchlet K was determined by measuring the flow rate into the stem and the water potential driving force. The flow rate (mmol s^{-1}) was measured using a custom-made flow meter where water is drawn from a reservoir through a tube attached to the cut stem of the branchlet and through a capillary tube of known conductance ($\text{mmol s}^{-1} \text{MPa}^{-1}$). Using an inline pressure transducer (PX-136; Omega Engineering Inc., Stamford, CT, USA), the change in pressure across the capillary tube was measured (values were logged using a Campbell Scientific CR 10 datalogger, (Campbell Scientific, Logan, UT, USA)) and a flow rate calculated (Brodrribb & Feild, 2000; Brodrribb, 2006; Brodrribb & Cochard, 2009). After the maximum flow was reached and began to decline, the stem was removed, wrapped in paper towel and plastic film, and left to equilibrate for *c.* 15 min before the branchlet water potential was measured using a Scholander pressure chamber. The maximum flow rate was divided by the water potential driving force (megapascals), measured before the stem was attached to the flow meter, to give branchlet conductivity as described in Brodrribb & Cochard (2009). The flow rate was normalized to 20°C and expressed per downstream leaf projected area (measured on a flatbed scanner) in $\text{mmol m}^{-2} \text{s}^{-1} \text{MPa}^{-1}$. The branchlet K was determined separately for each of the water potentials. The K values were then plotted to determine whether there was a difference in the K of the OVT prepared (cut) and nonprepared (uncut) branchlets. An ANOVA found no significant difference between the average hydraulic conductance K of cut and uncut branchlets at the two water potentials (-2 MPa and -5.5 MPa) ($P > 0.05$; Fig. S6).

Statistical analysis

The data were found to be normally distributed, and statistical significance was determined using linear mixed effect models in RSTUDIO v.4.0.2 (RStudio Team, 2016), with P50 or P88 as the

response and tree 'ID' and replicate (branchlet) as fixed effects. Specifically, we used the lmer function in the LME4 R package (Bates *et al.*, 2015). To account for repeated measures (pseudoreplication), we included tree ID as a random effect to satisfy the assumptions of a linear model (Harrison *et al.*, 2018). To test for differences in branchlet P50s and P88s within and among trees, we used the ANOVA function in the CAR R package (Fox & Weisberg, 2019). The breakpoint analysis was also conducted using RSTUDIO v.4.0.2 (RStudio Team, 2016). The remaining data were analysed using PYTHON v.3.9.1, and plots were constructed using SIGMAPLOT v.12.5 (Systat Software, 2003) and RSTUDIO (RStudio Team, 2016).

Results

Monitoring embolism *in vivo*

Xylem embolism spread was successfully monitored in three to five branchlets per tree across four *C. rhomboidea* saplings dried to different levels of water stress, with cameras attached to branchlets continuously capturing images for a total of 20–30 d per tree. Plants dehydrated slowly, taking 12–19 d to reach the three levels of water stress (mild, -4.4 and -4.9 MPa; moderate: -7.3 MPa; severe -9.5 MPa), after which they were rewatered (Fig. 2). Rehydration, to water potentials close to 0 MPa, took 1–3 d (24–72 h) per plant, which was followed by excision of branchlets, inducing rapid decline of branchlet water potential (calculated from branchlet shrinkage; Fig. 2). Decline of branchlet water potential ceased and 100% embolism was reached 1–5 d post-excision (Fig. 2).

Canopy embolism spread

Vulnerability to embolism Initial xylem embolism was recorded *in vivo* between 1 and 14 d across all plants after water was withheld. Once initiated, embolism spread in blocks caused by large numbers of neighbouring tracheids simultaneously filling with air. Blocks constituted between 10% and 90% of the total embolized pixel area within a single frame. Embolism spread in this fashion until plants were rewatered, whereupon embolism ceased or showed minimal (< 5%) increase. Continued embolism formation after rewatering was observed in only four out of the 16 branchlets and was generally associated with high levels of embolism and a failure to rehydrate upon rewatering.

The timing and progression of embolism varied widely, both within the branchlets of single trees (Fig. 3) and between branches of different heights across all trees (Fig. 4a). Vulnerability to embolism in all trees was also highly variable across all branchlets measured, with the branchlet water potential at which 50% and 88% of the xylem was embolized (P50 and P88) ranging from -1.4 to -9.8 MPa and from -1.9 to -14.4 MPa, respectively, with an average P50 of -5.1 MPa \pm 0.56 SE and an average P88 of -7.3 MPa \pm 0.8 SE. A linear mixed effects model followed by an ANOVA found no significant difference in the average P50s or P88s of different trees and ($P > 0.05$; Fig. S7). P50s and P88s were not significantly different within or between

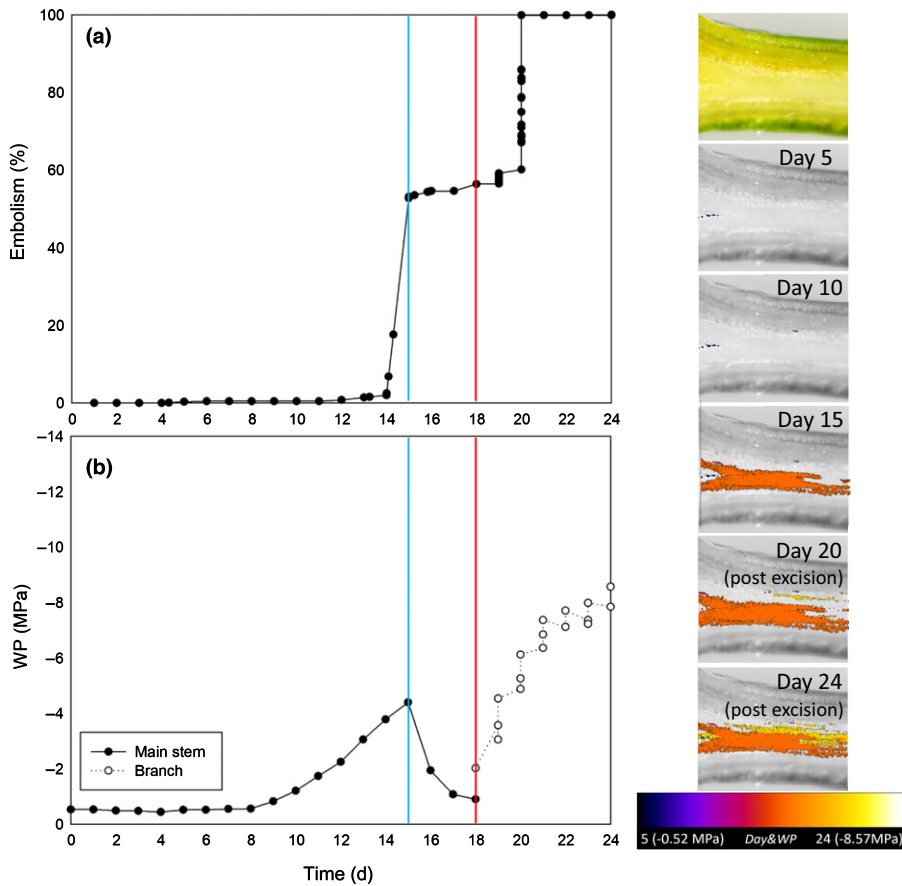


Fig. 2 (a) Percentage embolism and (b) water potential (WP) against time for a single branchlet of a *Callitris rhomboidea* sapling dried to -4.4 MPa, where the blue vertical line indicates where rewatering of the tree occurred and the red vertical line indicates when the branchlet was excised from the tree. The embolism data in (a) are calculated from images captured continuously, at 3-min intervals, with data points shown either once per day or where cavitation events were observed. The images in the right-hand column show (from the top) a raw image of the stem visualized using the optical vulnerability technique and visual representations of the embolism observed on day 5, day 10, day 15, day 20, and day 24 of embolism monitoring. Post-excision water potential was based on the relationship between water potential and branchlet shrinkage.

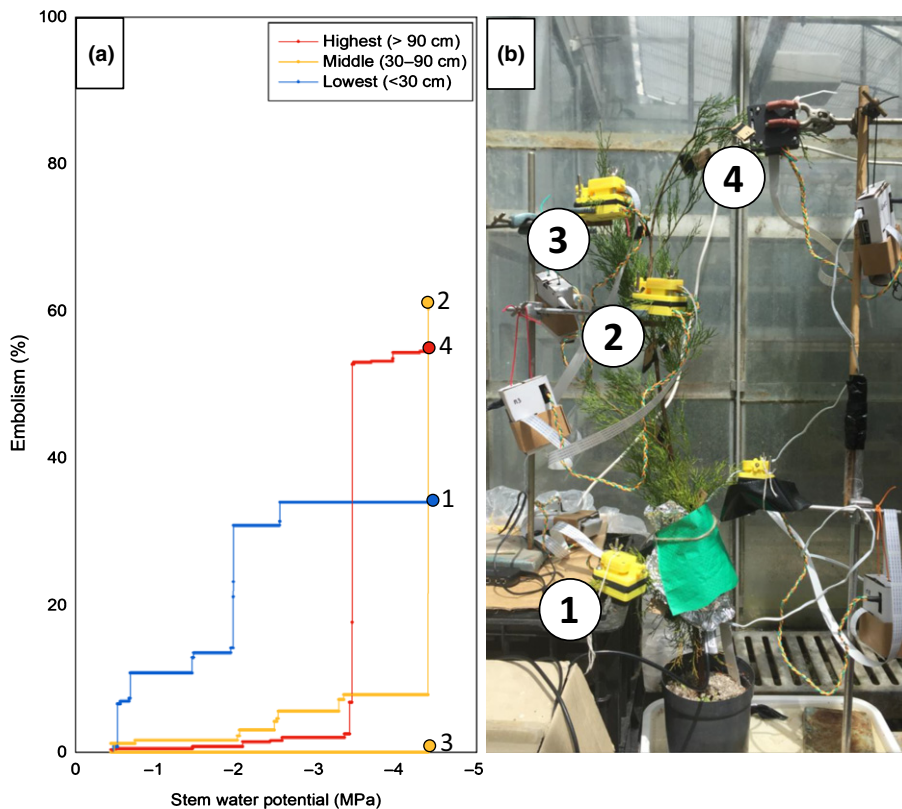


Fig. 3 An example of variable embolism spread during the drought treatment (where water potential was becoming increasingly negative) in the four branchlets monitored for embolism in a single *Callitris rhomboidea* tree (dried to -4.4 MPa). Branchlets in (a) are colour coded according to height and numbered (lowest branchlet, <30 cm, blue; middle branchlets, 30 – 90 cm, yellow; highest branchlet, >90 cm, red). In (b) their location is shown on the tree.

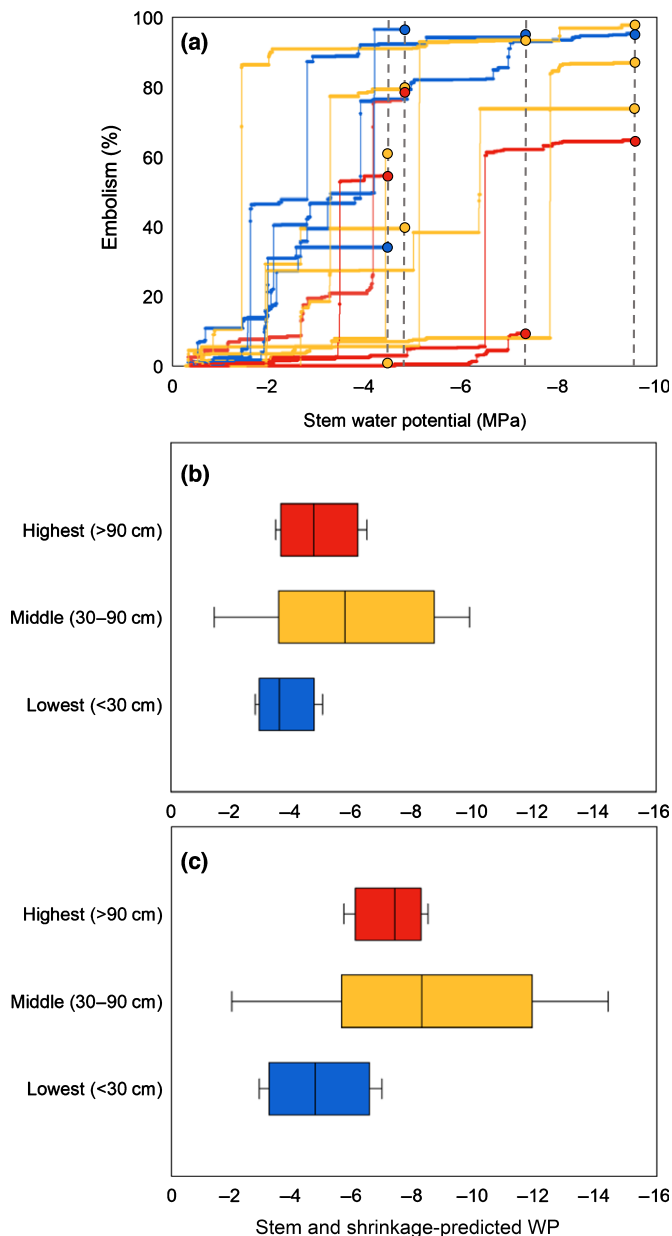


Fig. 4 Variation in embolism spread among all individuals was not associated with branch position. (a) Embolism that occurred during the drought treatments (where water potential was becoming increasingly negative) for each of the 16 branchlets against main-stem water potential. There were three to five branches per tree; the filled circles indicate the total embolism for each branchlet, and the vertical grey dashed lines represent each of the drought treatments (−4.4, −4.9, −7.3, −9.5 MPa). Branchlets are colour coded according to height (lowest branchlets, < 30 cm, blue; middle branchlets, 30–90 cm, yellow; highest branchlets, > 90 cm, red) in all panels. (b, c) The vertical lines in the panels show the median (b) P50 and (c) P88 for each of the height classes, with SE, using both main-stem water potential and predicted water potential values. The boxplots show the full range of the data. Where main-stem water potential could not be used, the water potential values for P50 and P88 were predicted from the relationship between branchlet shrinkage and main-stem water potential, which was averaged across all branchlets.

trees, but more variation was found within trees (ANOVA, $P=0.11$ and $P=0.15$) than between them ($P=0.94$ and $P=0.64$). Likewise, there was no significant difference in the P50

or P88 of the lowest branchlets (< 30 cm above the soil), middle branchlets (30–90 cm), and highest branchlets (> 90 cm) across all trees (ANOVA, $P>0.05$; Fig. 4b,c). These vulnerability data were supported by branchlet hydraulic data, where the percentage reduction in hydraulic conductance K between −2 and −5.5 MPa, based on calculated averages or the two water potentials, was 29% (Fig. S6) and corresponded with the OVT-detected average loss of branchlet xylem function between these water potentials (31%; Fig. S4).

Predicting canopy death

The mean branchlet-tip fluorescence (F_v/F_m) across all trees was 0.77 before drought and dropped to 0.7 ($P<0.05$) after drought when averaged across all but the severely stressed tree (dried to −9.5 MPa), with no significant differences between the F_v/F_m of branchlets that were monitored for embolism using the OVT and those that were not (Fig. S2). In the severely stressed tree, all post-drought fluorescence values were below 0.3 (Fig. S2).

Branchlets were found to tolerate up to 90% loss of xylem functional area due to embolism before the photosynthetic machinery was impacted (Fig. 5). Fluorescence (F_v/F_m) measurements indicate that beyond this 90% embolism threshold (in branchlets with between 90% and 99% embolized area) there was variation in whether branchlets incurred severe damage to the photosynthetic system. Fluorescence values were greater than 0.6 in the mildly stressed (−4.4 and −4.9 MPa) and moderately stressed (−7.3 MPa) trees, whereas all values were below 0.2 in the severely stressed tree (−9.5 MPa; Fig. 5).

In all but the most severely stressed tree (dried to −9.5 MPa), transpiration recovered to equal to or greater than predrought levels within 72 h after rewatering (Fig. S8). A reduction in transpiration post-drought was observed in the severely stressed tree (−9.5 MPa), where transpiration was $c.$ 33% of that measured predrought immediately after drought and took $c.$ 6 months to recover to predrought levels (Fig. S9). This reduction of transpiration was also associated with widespread damage to branch tips (Fig. 6b,c). All trees survived the drought treatments, with visible damage to the foliage occurring only in the most distal tips of the canopy foliage, which was minor in all but the severely stressed tree (Fig. 6).

Discussion

Experimentation on excised tissues has been fundamental to establishing principles of how xylem embolism jeopardizes plant survival, yet the absence of techniques allowing *in vivo* monitoring has limited our ability to understand the dynamics of drought-induced embolism propagation through intact plants. Here, we show how an optical technique can be used to monitor embolism continuously and nondestructively in living trees.

Continuous monitoring of xylem embolism in branchlets of *C. rhomboidea* saplings revealed exceedingly wide variation in branchlet vulnerability to embolism. Despite this variation, tissue

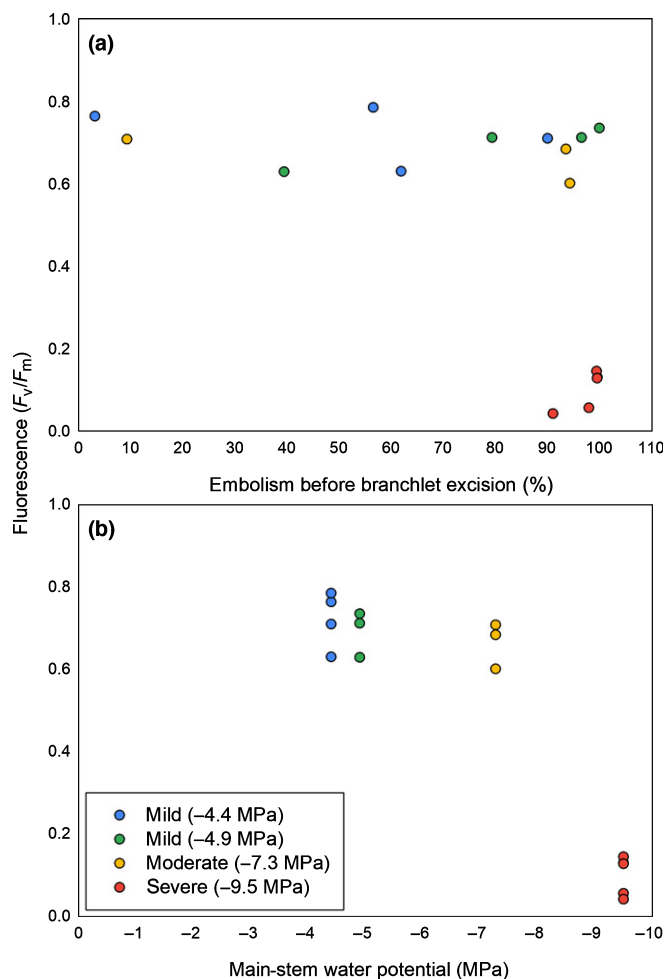


Fig. 5 The relationship between (a) percentage embolism and maximum quantum yield (fluorescence, F_v/F_m) after drought and rehydration, and (b) minimum water potential before rewetting and the fluorescence after drought and rehydration for each of the branchlets in which embolism was measured for the four *Callitris rhomboidea* saplings (mild, -4.4 MPa, blue; mild, -4.9 MPa, green; moderate, -7.3 MPa, yellow; severe, -9.5 MPa, red).

damage was consistently linked to cavitation of $\geq 90\%$, suggesting high resistance to tissue death in the terminal parts of the xylem of this conifer species.

Runaway cavitation and tissue death

For tissue death during drought to be causally related to cavitation by the process of runaway cavitation we would expect



Fig. 6 Tip death representative of that observed in *Callitris rhomboidea* saplings dried to mild (-4.4 and -4.9 MPa) and moderate (-7.3 MPa) level of water stress, post experimentation (a) and the severely stressed tree (dried to -9.5 MPa) (b) immediately after drought and (c) 2 months after drought.

damage to occur downstream of xylem suffering nearly 100% embolism (Milburn, 1973; Tyree & Sperry, 1988). This is because the rate of water loss after stomatal closure is very low, meaning a large loss of hydraulic conductance K would be required to disrupt the homeostatic water balance in leaves (leading to a local drop in water potential and runaway cavitation). However, at close to 100% embolism, where K is small, even a tiny amount of water loss could disrupt this balance, triggering a positive feedback between xylem cavitation and falling water potential leading to rapid tissue desiccation and death (Brodrribb *et al.*, 2021). Therefore, if runaway cavitation causes tissue death, it likely occurs at very high embolism percentages starting at the leaves, as they are the primary site of plant water loss and often the most vulnerable plant organ (Charrier *et al.*, 2016; Skelton *et al.*, 2019).

Our data provide some support for the idea that runaway cavitation at high percentages of embolism is a primary trigger of tissue desiccation in the distal leaf tissue of *C. rhomboidea* branchlets. Here, we assume that branchlet xylem function can be restored by xylem refilling, which is supported by a number of studies that show this is rare in trees (Cochard *et al.*, 2013; Charrier *et al.*, 2016; Lamarque *et al.*, 2018). We found that severe damage to the photosynthetic machinery only occurred in branchlets with $> 90\%$ embolized area, providing some evidence that runaway cavitation is responsible for tissue death. However, providing unequivocal support for this link is difficult due to the interplay between percentage loss of conductance and environmental conditions. Under certain circumstances, such as very hot days where percentage stem embolism is $\geq 90\%$ and leaf transpiration is high, tissue death would occur rapidly once the runaway cavitation feedback was initiated, making the timing of runaway cavitation unpredictable and a causal link between runaway cavitation and tissue death difficult to capture. It is also worth noting that recovery of photosynthetic function may be observed longer term by the regrowth of new xylem, a mechanism known to facilitate drought recovery in *C. rhomboidea* (Brodrribb *et al.*, 2010). Recently, a direct link between runaway cavitation and tissue death has been found in tomato leaves, supporting the idea of this causal link at the terminal parts of other plant vascular systems (Brodrribb *et al.*, 2021).

Our finding that a high percentage of embolism is required to induce downstream tissue damage aligns with previous findings in conifer leaves (Brodrribb & Cochard, 2009; Choat, 2013; Liang *et al.*, 2021), but it contrasts with research in wheat leaves, where tissue damage occurred at much lower embolism percentages (Johnson *et al.*, 2018). Grasses and trees are, indeed,

different in many ways, and a possible explanation for the contrast in the onset of tissue damage may be differences in foliar carbon (C) investment, as conifers like *C. rhomboidea* produce long-lived leaves with a high C 'cost', whereas grass leaves are usually comparatively short-lived and lower 'cost'. Additionally, many grasses possess basal meristems, which may be more drought resistant than the leaves and able to produce new leaves after drought (Volaire *et al.*, 2009, 2018; Johnson *et al.*, 2018). The higher C 'cost' of leaves (or, in the case of *C. rhomboidea*, branchlets) may explain why conifers appear to sustain leaves until runaway cavitation drives lethal desiccation, whereas leaf damage occurs well before runaway cavitation in grass leaves, which may be driven by drought-stress-induced senescence (Rivero *et al.*, 2007). This raises an interesting possibility, that the cost of replacing tissues, tissue longevity, or life strategy may influence the extent of embolism at the point of tissue death in plants, an idea to consider when interpreting species vulnerability to drought-induced embolism.

Variation in branchlet vulnerability to embolism

Vulnerability to drought-induced xylem embolism was surprisingly variable among the 16 branchlets measured across four *C. rhomboidea* saplings. Though variation in xylem vulnerability has been found between individuals within a species (Wortemann *et al.*, 2011; Anderegg, 2015; Stojnić *et al.*, 2018) and even within the leaves of a single canopy (Rodríguez-Domínguez *et al.*, 2018; Cardoso *et al.*, 2020), the range of vulnerabilities found here was unexpected. Despite the very wide range of branchlet P50s, the average P50 of $-5.1 \text{ MPa} \pm 0.56 \text{ SE}$ was similar to the previously reported P50 for *C. rhomboidea* branchlets of -6.60 MPa , but less than that previously reported in stems of -10 MPa (Brodrribb & Cochard, 2009; Larter *et al.*, 2017). As the previously reported leaf P50 was calculated in small (2 mm diameter) branchlets (like those monitored here) and the stem P50 was calculated using larger, older branchlets (10 mm diameter), this suggests significant vulnerability scaling within branches (Brodrribb & Cochard, 2009).

Owing to the unexpectedly high range in branch vulnerability, we were careful to eliminate methodological error as a source of this variability by, first, ensuring branchlet preparation (i.e. opening a small window in the bark with a sharp razor blade) did not affect photosynthetic or hydraulic function and, second, by using hydraulic data to verify the optical method. The increase in percentage embolism found with OVT between -2 MPa and -5 MPa matched closely with the percentage loss of conductance found between these water potentials using hydraulic measurements (Fig. S6). Furthermore, we note that the OVT has been shown to accurately represent embolism formation in small woody stems (Johnson *et al.*, 2020) and that the reliability of the optical technique has been shown through numerous comparisons with traditional hydraulic methods and X-ray imagery (Brodrribb *et al.*, 2016b; Skelton *et al.*, 2018; Gauthey *et al.*, 2020; Johnson *et al.*, 2020). Also, optical vulnerability measurements in stems show much lower variation between individuals than in leaves (Rodríguez-Domínguez *et al.*, 2018; Cardoso *et al.*, 2020),

suggesting that the variation we observed here might be characteristic of the terminal parts of the vascular system. Through the high temporal resolution provided by continuous monitoring, the optical technique enables us to capture the true variability in embolism within plants. The questions that remain, then, are as follows: What is controlling the large variation between branchlets? What does it mean for the response of *C. rhomboidea* trees to drought? Does it form part of a strategy for drought resistance in this drought-tolerant conifer?

Explaining high variability among branchlets

The large variation in branchlet vulnerability indicates a wide range of tracheid vulnerabilities in this species, and a nonrandom distribution of this possible range within branchlets may explain the variation between them. Research in stems has found that neighbouring conduits are more likely to cavitate together (Mrad *et al.*, 2018, 2020; Johnson *et al.*, 2020) and that the vulnerability of xylem may be linked to the ontogenetic stage of the plant (Fontes & Cavender-Bares, 2020) or the age of growth rings (Choat *et al.*, 2015; Fukuda *et al.*, 2015), suggesting that xylem conduits produced at the same time, and therefore under similar conditions, may have similar cavitation vulnerability.

As trees grow continuously, we propose that differences in the environmental conditions at the time of branchlet growth may lead to variation in the vulnerability of their xylem. Xylem plasticity in response to environmental conditions has been found in *Helianthus annuus* leaves and *Pinus pinaster* stems, where xylem embolism resistance increased in water-limited conditions (Corcuera *et al.*, 2011; Cardoso *et al.*, 2018); similarly, summer drought was found to increase traits conferring drought tolerance in tree rings of *Larix decidua* and *Picea abies* (Bryukhanova & Fonti, 2013). High light exposure has also been linked to increased embolism resistance in *Fagus sylvatica* leaves and *Populus nigra* stems (Cochard *et al.*, 1999; Herbette *et al.*, 2010; Tomasella *et al.*, 2021). This suggests that xylem produced under water-limited conditions, and increased sunlight (e.g. summer), may be more resistant to embolism than that produced in well-watered conditions (e.g. spring and winter). As such, seasonal differences at the time of branchlet extension may have resulted in similar tracheid vulnerabilities within branchlets, but differences between them, contributing to variable vulnerability to embolism between branchlets.

The highly variable branchlet vulnerability found here may represent an adaptive strategy to prevent sudden catastrophic damage to the tree canopy during drought. As noted by Cardoso *et al.* (2020), many species with high variability in leaf vulnerability are also highly drought resistant (Johnson *et al.*, 2018; Lamarque *et al.*, 2018; Rodríguez-Domínguez & Brodrribb, 2020), which is also true of *C. rhomboidea* (Brodrribb & Cochard, 2009). In trees with variable leaf or terminal branchlet vulnerabilities, lethal embolism and tissue death would likely occur gradually across the canopy during drought. This gradual loss of branchlets, and therefore of leaf area, may serve as a strategy to slow the rate of dehydration by reducing water lost through transpiration as described by 'the hydraulic fuse' hypothesis and the theory of 'branch sacrifice', referring to leaf shedding and branchlet loss

during drought (Tyree & Sperry, 1988; Rood *et al.*, 2000; Wolfe *et al.*, 2016). This idea relies on a trade-off associated with producing embolism-resistant xylem. We propose that this may be related to growth rate, where faster growth rates lead to more vulnerable xylem and slower growth rates lead to more resistant xylem. By preventing rapid and catastrophic cavitation damage to the entire canopy, this strategy would also enable trees to recover some photosynthetic capacity post-drought, increasing their chance of survival. These ideas require further investigation, including research to determine whether growth rate is in fact related to xylem vulnerability in *C. rhomboidea* branchlets.

Conclusions

By tracking embolism spread in branchlets of *C. rhomboidea* trees during long-term drought treatments, we revealed high variation in embolism vulnerability and high resistance of branchlets to tissue damage. The differences in branchlet vulnerability indicate large variation in tracheid vulnerabilities, which may be driven by differences in the conditions during branchlet extension. This variation may also form part of a strategy that enables drought-resistant trees like *C. rhomboidea* to survive drought through gradual branchlet sacrifice. Measurements of photosynthetic capacity as a proxy for tissue vitality showed that branchlets could withstand xylem failure of $\geq 90\%$ before tissue damage, providing some evidence for a causal link between runaway cavitation and tissue death in *C. rhomboidea* branchlets. By utilizing techniques to monitor embolism and tissue death *in vivo*, we inch closer to pinpointing the mechanisms that drive drought-induced death and confer drought survival in trees and all plants.

Acknowledgements

We thank Brad Johnson for his assistance with PYTHON software. This research was supported by the Department of Industry, Innovation, Science, Research and Tertiary Education of the Australian Government Research (Training Program Scholarship to KMJ), the Australian Research Council (grant no. DP190101552), The ARC Centre of Excellence for Plant Success in Nature and Agriculture (CE200100015), and the Holsworth Wildlife Research Endowment & The Ecological Society of Australia.

Author contributions

TJB and KMJ conceived the concept for this research and designed the experiments. CL designed the method for data storage and collection during embolism monitoring. KMJ conducted the experiments and collected and analysed data, which was interpreted by both KMJ and TJB. KMJ wrote the manuscript with significant contribution from TJB and contribution from CL.

ORCID

Timothy J. Brodribb  <https://orcid.org/0000-0002-4964-6107>
 Kate M. Johnson  <https://orcid.org/0000-0002-3039-6339>
 Christopher Lucani  <https://orcid.org/0000-0001-8983-3575>

Data availability

The data that support the findings of this study are available from the corresponding authors upon reasonable request.

References

- Allen CD, Macalady AK, Chenchouni H, Bachelet D, McDowell N, Vennetier M, Kitzberger T, Rigling A, Breshears DD, Hogg EH *et al.* 2010. A global overview of drought and heat-induced tree mortality reveals emerging climate change risks for forests. *Forest Ecology and Management* 259: 660–684.
- Anderegg WRL. 2015. Spatial and temporal variation in plant hydraulic traits and their relevance for climate change impacts on vegetation. *New Phytologist* 205: 1008–1014.
- Bates D, Maechler M, Bolker B, Walker S. 2015. Fitting linear mixed-effects models using lme4. *Journal of Statistical Software* 67: 1–48.
- Becker M, Kerstiens G, Schönherr J. 1986. Water permeability of plant cuticles: permeance, diffusion and partition coefficients. *Trees* 1: 54–60.
- Blackman CJ, Brodribb TJ, Jordan GJ. 2012. Leaf hydraulic vulnerability influences species' bioclimatic limits in a diverse group of woody angiosperms. *Oecologia* 168: 1–10.
- Blackman CJ, Pfausch S, Choat B, Delzon S, Gleason SM, Duursma RA. 2016. Toward an index of desiccation time to tree mortality under drought. *Plant, Cell & Environment* 39: 2342–2345.
- Bouche PS, Larter M, Domec J-C, Burell R, Gasson P, Jansen S, Delzon S. 2014. A broad survey of hydraulic and mechanical safety in the xylem of conifers. *Journal of Experimental Botany* 65: 4419–4431.
- Bourbia I, Carins-Murphy MR, Gracie A, Brodribb TJ. 2020. Xylem cavitation isolates leaky flowers during water stress in pyrethrum. *New Phytologist* 227: 146–155.
- Bourbia I, Pritzkow C, Brodribb TJ. 2021. Herb and conifer roots show similar high sensitivity to water deficit. *Plant Physiology* 186: 1908–1918.
- Brodribb TJ, Bienaimé D, Marmottant P. 2016a. Revealing catastrophic failure of leaf networks under stress. *Proceedings of the National Academy of Sciences, USA* 113: 4865–4869.
- Brodribb TJ, Bowman DJMS, Nichols S, Delzon S, Burell R. 2010. Xylem function and growth rate interact to determine recovery rates after exposure to extreme water deficit. *New Phytologist* 188: 533–542.
- Brodribb T, Brodersen CR, Carriqui M, Tonet V, Rodriguez Dominguez C, McAdam S. 2021. Linking xylem network failure with leaf tissue death. *New Phytologist* 232: 68–79.
- Brodribb TJ, Carriqui M, Delzon S, Lucani C. 2017. Optical measurement of stem xylem vulnerability. *Plant Physiology* 174: 2054–2061.
- Brodribb TJ, Cochard H. 2009. Hydraulic failure defines the recovery and point of death in water-stressed conifers. *Plant Physiology* 149: 575–584.
- Brodribb TJ, Feild TS. 2000. Stem hydraulic supply is linked to leaf photosynthetic capacity: evidence from New Caledonian and Tasmanian rainforests. *Plant, Cell & Environment* 23: 1381–1388.
- Brodribb TJ, Holbrook NM. 2006. Declining hydraulic efficiency as transpiring leaves desiccate: two types of response. *Plant, Cell & Environment* 29: 2205–2215.
- Brodribb TJ, McAdam SAM. 2017. Evolution of the stomatal regulation of plant water content. *Plant Physiology* 174: 639.
- Brodribb TJ, Powers J, Cochard H, Choat B. 2020. Hanging by a thread? Forests and drought. *Science* 368: 261–266.
- Brodribb TJ, Skelton RP, McAdam SA, Bienaimé D, Lucani CJ, Marmottant P. 2016b. Visual quantification of embolism reveals leaf vulnerability to hydraulic failure. *New Phytologist* 209: 1403–1409.
- Bryukhanova M, Fonti P. 2013. Xylem plasticity allows rapid hydraulic adjustment to annual climatic variability. *Trees* 27: 485–496.
- Cardoso AA, Batz TA, McAdam SAM. 2020. Xylem embolism resistance determines leaf mortality during drought in *Persea americana*. *Plant Physiology* 182: 547–554.
- Cardoso AA, Brodribb TJ, Lucani CJ, DaMatta FM, McAdam SAM. 2018. Coordinated plasticity maintains hydraulic safety in sunflower leaves. *Plant, Cell & Environment* 41: 2567–2576.

- Charrier G, Torres-Ruiz JM, Badel E, Burlett R, Choat B, Cochard H, Delmas CEL, Domec JC, Jansen S, King A *et al.* 2016. Evidence for hydraulic vulnerability segmentation and lack of xylem refilling under tension. *Plant Physiology* 172: 1657–1668.
- Choat B. 2013. Predicting thresholds of drought-induced mortality in woody plant species. *Tree Physiology* 33: 669–671.
- Choat B, Badel E, Burlett R, Delzon S, Cochard H, Jansen S. 2016. Noninvasive measurement of vulnerability to drought-induced embolism by X-ray microtomography. *Plant Physiology* 170: 273–282.
- Choat B, Brodersen CR, McElrone AJ. 2015. Synchrotron X-ray microtomography of xylem embolism in *Sequoia sempervirens* saplings during cycles of drought and recovery. *New Phytologist* 205: 1095–1105.
- Choat B, Jansen S, Brodribb TJ, Cochard H, Delzon S, Bhaskar R, Buccini SJ, Feild TS, Gleason SM, Hacke UG *et al.* 2012. Global convergence in the vulnerability of forests to drought. *Nature* 491: 752–755.
- Cochard H, Badel E, Herbette S, Delzon S, Choat B, Jansen S. 2013. Methods for measuring plant vulnerability to cavitation: a critical review. *Journal of Experimental Botany* 64: 4779–4791.
- Cochard H, Delzon S, Badel E. 2015. X-ray microtomography (micro-CT): a reference technology for high-resolution quantification of xylem embolism in trees. *Plant, Cell & Environment* 38: 201–206.
- Cochard H, Lemoine D, Dreyer E. 1999. The effects of acclimation to sunlight on the xylem vulnerability to embolism in *Fagus sylvatica* L. *Plant, Cell & Environment* 22: 101–108.
- Corcuera L, Cochard H, Gil-Pelegrin E, Notivol E. 2011. Phenotypic plasticity in mesic populations of *Pinus pinaster* improves resistance to xylem embolism (P₅₀) under severe drought. *Trees* 25: 1033–1042.
- Dietrich L, Hoch G, Kahmen A, Körner C. 2018. Losing half the conductive area hardly impacts the water status of mature trees. *Scientific Reports* 8: e15006.
- Duursma RA, Blackman CJ, López R, Martin-StPaul NK, Cochard H, Medlyn BE. 2019. On the minimum leaf conductance: its role in models of plant water use, and ecological and environmental controls. *New Phytologist* 221: 693–705.
- Fontes CG, Cavender-Bares J. 2020. Toward an integrated view of the ‘elephant’: unlocking the mysteries of water transport and xylem vulnerability in oaks. *Tree Physiology* 40: 1–4.
- Fox J, Weisberg S. 2019. *An R companion to applied regression, 3rd edn.* Thousand Oaks, CA, USA: Sage.
- Fukuda K, Kawaguchi D, Aihara T, Ogasa MY, Miki NH, Haishi T, Umebayashi T. 2015. Vulnerability to cavitation differs between current-year and older xylem: non-destructive observation with a compact magnetic resonance imaging system of two deciduous diffuse-porous species. *Plant, Cell & Environment* 38: 2508–2518.
- Gauthey A, Peters JMR, Carins-Murphy MR, Rodriguez-Dominguez CM, Li X, Delzon S, King A, López R, Medlyn BE, Tissue DT *et al.* 2020. Visual and hydraulic techniques produce similar estimates of cavitation resistance in woody species. *New Phytologist* 228: 884–897.
- Hammond WM, Yu K, Wilson LA, Will RE, Anderegg WRL, Adams HD. 2019. Dead or dying? Quantifying the point of no return from hydraulic failure in drought-induced tree mortality. *New Phytologist* 223: 1834–1843.
- Harrison XA, Donaldson L, Correa-Cano ME, Evans J, Fisher DN, Goodwin CED, Robinson BS, Hodgson DJ, Inger R. 2018. A brief introduction to mixed effects modelling and multi-model inference in ecology. *PeerJ* 6: e4794.
- Heady RD, Cunningham RB, Donnelly CF, Evans PD. 1994. Morphology of warts in the tracheids of cypress pine (*Callitris* Vent.). *LAWA Journal* 15: 265–281.
- Herbette S, Wortemann R, Awad H, Huc R, Cochard H, Barigah TS. 2010. Insights into xylem vulnerability to cavitation in *Fagus sylvatica* L.: phenotypic and environmental sources of variability. *Tree Physiology* 30: 1448–1455.
- Hochberg U, Windt CW, Ponomarenko A, Zhang Y-J, Gersony J, Rockwell FE, Holbrook NM. 2017. Stomatal closure, basal leaf embolism, and shedding protect the hydraulic integrity of grape stems. *Plant Physiology* 174: 764–775.
- Hoegh-Guldberg O, Jacob D, Taylor M, Bindi M, Brown N, Camilloni I, Diedhiou A, Djalante R, Ebi KL, Engelbrecht F *et al.* 2018. Impacts of 1.5°C global warming on natural and human systems. In: Masson-Delmotte V, Zhai P, Pörtner H-O, Roberts D, Skea J, Shukla PR, Pirani A, Moufouma-Okia W, Péan C, Pidcock R *et al.*, eds. *Global warming of 1.5°C. An IPCC Special Report on the impacts of global warming of 1.5°C above pre-industrial levels and related global greenhouse gas emission pathways, in the context of strengthening the global response to the threat of climate change, sustainable development, and efforts to eradicate poverty*, in press. https://www.ipcc.ch/site/assets/uploads/sites/2/2019/06/SR15_Full_Report_High_Res.pdf
- Johnson KM, Brodersen CR, Carins-Murphy MR, Choat B, Brodribb TJ. 2020. Xylem embolism spreads by single-conduit events in three dry forest angiosperm stems. *Plant Physiology* 184: 212–222.
- Johnson KM, Jordan GJ, Brodribb TJ. 2018. Wheat leaves embolized by water stress do not recover function upon rewetting. *Plant, Cell & Environment* 41: 2704–2714.
- Kerstiens G. 1996. The cuticle of early vascular plants and its evolutionary significance. *Journal of Experimental Botany* 47: 1813–1832.
- Lamacque L, Charrier G, dos Santos Farnese F, Lemaire B, Améglio T, Herbette S. 2020. Drought-induced mortality: branch diameter variation reveals a point of no recovery in lavender species. *Plant Physiology* 183: 1638.
- Lamarque LJ, Corso D, Torres-Ruiz JM, Badel E, Brodribb TJ, Burlett R, Charrier G, Choat B, Cochard H, Gambetta GA *et al.* 2018. An inconvenient truth about xylem resistance to embolism in the model species for refilling *Laurus nobilis* L. *Annals of Forest Science* 75: e88.
- Larter M, Pfautsch S, Domec JC, Trueba S, Nagalingum N, Delzon S. 2017. Aridity drove the evolution of extreme embolism resistance and the radiation of conifer genus *Callitris*. *New Phytologist* 215: 97–112.
- Lenzian KJ, Kerstiens G. 1991. Sorption and transport of gases and vapors in plant cuticles. In: Ware GW, ed. *Reviews of environmental contamination and toxicology*. New York, NY, USA: Springer, 65–128.
- Lewis A. 1988. A test of the air-seeding hypothesis using *Sphagnum* hyalocysts. *Plant Physiology* 87: 577–582.
- Liang X, Ye Q, Liu H, Brodribb TJ. 2021. Wood density predicts mortality threshold for diverse trees. *New Phytologist* 229: 3053–3057.
- Márquez DA, Stuart-Williams H, Farquhar GD. 2021. An improved theory for calculating leaf gas exchange more precisely accounting for small fluxes. *Nature Plants* 7: 317–326.
- Martin-StPaul N. 2017. Plant resistance to drought depends on timely stomatal closure. *Ecology Letters* 29: 1437–1447.
- McDowell NG, Allen CD, Anderson-Teixeira K, Aukema BH, Bond-Lamberty B, Chini L, Clark JS, Dietze M, Grossiord C, Hanbury-Brown A *et al.* 2020. Pervasive shifts in forest dynamics in a changing world. *Science* 368: eaaz9463.
- McDowell NG, Ryan MG, Zeppel MJB, Tissue DT. 2013. Feature: improving our knowledge of drought-induced forest mortality through experiments, observations, and modeling. *New Phytologist* 200: 289–293.
- Melcher PJ, Holbrook NM, Burns MJ, Zwieniecki MA, Cobb AR, Brodribb TJ, Choat B, Sack L. 2012. Measurements of stem xylem hydraulic conductivity in the laboratory and field. *Methods in Ecology and Evolution* 3: 685–694.
- Milburn JA. 1973. Cavitation studies on whole *Ricinus* plants by acoustic detection. *Planta* 112: 333–342.
- Mrad A, Domec J-C, Huang C-W, Lens F, Katul G. 2018. A network model links wood anatomy to xylem tissue hydraulic behaviour and vulnerability to cavitation. *Plant, Cell & Environment* 41: 2718–2730.
- Mrad A, Johnson DM, Love DM, Domec J-C. 2020. The roles of conduit redundancy and connectivity in xylem hydraulic functions. *New Phytologist* 231: 996–1007.
- Muggeo V. 2008. SEGMENTED: an R package to fit regression models with broken-line relationships. *R News* 8, 20–25 (CRAN).
- Nardini A, Savi T, Losso A, Petit G, Pacilè S, Tromba G, Mayr S, Trifilò P, Lo Gullo MA, Salleo S. 2017. X-ray microtomography observations of xylem embolism in stems of *Laurus nobilis* are consistent with hydraulic measurements of percentage loss of conductance. *New Phytologist* 213: 1068–1075.
- Nolf M, Lopez R, Peters JMR, Flavel RJ, Kolodzin LS, Young IM, Choat B. 2017. Visualization of xylem embolism by X-ray microtomography: a direct test against hydraulic measurements. *New Phytologist* 214: 890–898.
- Petrzellis F, Pagliarini C, Savi T, Losso A, Cavalletto S, Tromba G, Dullin C, Bär A, Ganthaler A, Miotto A *et al.* 2018. The pitfalls of *in vivo* imaging techniques: evidence for cellular damage caused by synchrotron X-ray computed micro-tomography. *New Phytologist* 220: 104–110.
- Pittermann J, Choat B, Jansen S, Stuart SA, Lynn L, Dawson TE. 2010. The relationships between xylem safety and hydraulic efficiency in the Cupressaceae:

- the evolution of pit membrane form and function. *Plant Physiology* 153: 1919–1931.
- Preisler Y, Tatarinov F, Gruüzweig JM, Yakir D. 2020. Seeking the 'point of no return' in the sequence of events leading to mortality of mature trees. *Plant, Cell & Environment* 44: 1315–1328.
- Rivero RM, Kojima M, Gepstein A, Sakakibara H, Mittler R, Gepstein S, Blumwald E. 2007. Delayed leaf senescence induces extreme drought tolerance in a flowering plant. *Proceedings of the National Academy of Sciences, USA* 104: 19631–19636.
- Rodriguez-Dominguez CM, Brodrribb TJ. 2020. Declining root water transport drives stomatal closure in olive under moderate water stress. *New Phytologist* 225: 126–134.
- Rodriguez-Dominguez CM, Carins Murphy MR, Lucani C, Brodrribb TJ. 2018. Mapping xylem failure in disparate organs of whole plants reveals extreme resistance in olive roots. *New Phytologist* 218: 1025–1035.
- Rood SB, Patiño S, Coombs K, Tyree MT. 2000. Branch sacrifice: cavitation-associated drought adaptation of riparian cottonwoods. *Trees* 14: 248–257.
- van Rossum G. 1995. *Python tutorial, Technical Report CS-R9526*. Amsterdam, the Netherlands: Centrum voor Wiskunde en Informatica (CWI).
- RStudio Team. 2016. *RSTUDIO: integrated development for R*. Boston, MA, USA: RStudio PBC. [WWW document] URL <http://www.rstudio.com/>.
- Skelton RP, Anderegg LDL, Papper P, Reich E, Dawson TE, Kling M, Thompson SE, Diaz J, Ackerly DD. 2019. No local adaptation in leaf or stem xylem vulnerability to embolism, but consistent vulnerability segmentation in a North American oak. *New Phytologist* 223: 1296–1306.
- Skelton RP, Brodrribb TJ, Choat B. 2017. Casting light on xylem vulnerability in an herbaceous species reveals a lack of segmentation. *New Phytologist* 214: 561–569.
- Skelton RP, Dawson TE, Thompson SE, Shen Y, Weitz AP, Ackerly D. 2018. Low vulnerability to xylem embolism in leaves and stems of North American oaks. *Plant Physiology* 177: 1066–1077.
- Skelton RP, West AG, Dawson TE. 2015. Predicting plant vulnerability to drought in biodiverse regions using functional traits. *Proceedings of the National Academy of Sciences, USA* 112: 5744–5749.
- Stojnić S, Suchocka M, Benito-Garzón M, Torres-Ruiz JM, Cochard H, Bolte A, Coccozza C, Cvjetković B, de Luis M, Martínez-Vilalta J *et al.* 2018. Variation in xylem vulnerability to embolism in European beech from geographically marginal populations. *Tree Physiology* 38: 173–185.
- Systat Software Inc. 2003. *SIGMAPLOT*. San Jose, CA, USA: Systat Software.
- Tomasella M, Casolo V, Natale S, Petruzzellis F, Kofler W, Beikircher B, Mayr S, Nardini A. 2021. Shade-induced reduction of stem nonstructural carbohydrates increases xylem vulnerability to embolism and impedes hydraulic recovery in *Populus nigra*. *New Phytologist* 231: 108–121.
- Tyree MT, Sperry JS. 1988. Do woody plants operate near the point of catastrophic xylem dysfunction caused by dynamic water stress? *Plant Physiology* 88: 574–580.
- Urli M, Porté AJ, Cochard H, Guengant Y, Burlett R, Delzon S. 2013. Xylem embolism threshold for catastrophic hydraulic failure in angiosperm trees. *Tree Physiology* 33: 672–683.
- Volaire F, Lens F, Cochard H, Xu H, Chacon-Doria L, Bristiel P, Balachowski J, Rowe N, Violle C, Picon-Cochard C. 2018. Embolism and mechanical resistances play a key role in dehydration tolerance of a perennial grass *Dactylis glomerata* L. *Annals of Botany* 122: 325–336.
- Volaire F, Seddaiu G, Ledda L, Lelievre F. 2009. Water deficit and induction of summer dormancy in perennial Mediterranean grasses. *Annals of Botany* 103: 1337–1346.
- Wang W, English NB, Grossiord C, Gessler A, Das AJ, Stephenson NL, Baisan CH, Allen CD, McDowell NG. 2021. Mortality predispositions of conifers across western USA. *New Phytologist* 229: 831–844.
- Wolfe BT, Sperry JS, Kursar TA. 2016. Does leaf shedding protect stems from cavitation during seasonal droughts? A test of the hydraulic fuse hypothesis. *New Phytologist* 212: 1007–1018.
- Wood S. 2011. Package "MGCV": mixed GAM computation vehicle with GCV/AIC/REML smoothness estimation and GAMMs. [WWW document] URL REML/PQL.cran.r-project.org/web/packages/mgcv/mgcv.pdf.
- Wortemann R, Herbette S, Barigah TS, Fumanal B, Alia R, Ducousso A, Gomory D, Roeckel-Drevet P, Cochard H. 2011. Genotypic variability and phenotypic plasticity of cavitation resistance in *Fagus sylvatica* L. across Europe. *Tree Physiology* 31: 1175–1182.
- Zhang F-P, Brodrribb TJ. 2017. Are flowers vulnerable to xylem cavitation during drought? *Proceedings of the Royal Society B: Biological Sciences* 284: e20162642.

Supporting Information

Additional Supporting Information may be found online in the Supporting Information section at the end of the article.

Fig. S1 Decrease in stem water potential (MPa) against time in each of the trees for the duration of the drought treatments.

Fig. S2 Branch tip maximum quantum yield of PS II (F_v/F_m) before and after drought in the measured branchlets of all trees.

Fig. S3 Xylem vulnerability curves for each of the branchlets monitored for embolism across the four trees.

Fig. S4 The relationship between stem water potential (MPa) and percentage branchlet shrinkages for all 16 branchlets monitored for embolism across the four trees.

Fig. S5 An example of the two branchlet preparation methods for hydraulic conductance (K) measurements used to test the effect of Optical Vulnerability Technique preparation of xylem function.

Fig. S6 Hydraulic Conductance (K) for branchlets of a single *Callitris rhomboidea* sapling where some branchlets were prepared as they would be for embolism visualisation using the Optical Vulnerability Technique and others were not.

Fig. S7 The median P50s and P88s with standard error for each of the four trees.

Fig. S8 Transpiration for all trees *c.* 3 d after rewatering post drought treatment as a percentage of the predrought (well-watered) transpiration.

Fig. S9 Transpiration for the severely stressed tree (dried to -9.5 MPa) 3 d, 2 months and 6 months after rewatering (post drought treatment) as a percentage of the predrought (well-watered) transpiration.

Video S1 Showing 5 MiCAMs attached to branchlets spanning the height of a *Callitris rhomboidea* sapling, taking images every 3 min, representing the set-up for drought-induced embolism monitoring in this study.

Please note: Wiley Blackwell are not responsible for the content or functionality of any Supporting Information supplied by the authors. Any queries (other than missing material) should be directed to the *New Phytologist* Central Office.